Elasticity of Single Polyelectrolyte Chains and Their Desorption from Solid Supports Studied by AFM Based Single Molecule Force Spectroscopy

Thorsten Hugel,[†] Matthias Grosholz,[†] Hauke Clausen-Schaumann,[†] Andreas Pfau,[‡] Hermann Gaub,[†] and Markus Seitz*,[†]

Lehrstuhl für Angewandte Physik & Center for NanoScience, Ludwig-Maximilians Universität, Amalienstrasse 54, 80799 München, Germany, and Polymer Research Division, BASF-AG, 67056 Ludwigshafen, Germany

Received May 30, 2000; Revised Manuscript Received November 7, 2000

ABSTRACT: AFM based single molecule force spectroscopy was used for the investigation of single polyelectrolyte chains. Namely, the elasticity of polyvinylamine chains and their desorption from solid surfaces was studied as a function of the polymer's charge density and electrolyte concentration. Experimental force−distance profiles were fitted by the wormlike chain model, including elastic contributions arising from the stretching of bond angles and covalent bonds. It was found that, under the high stretching forces which can be applied in the AFM experiments, the bending rigidity of polyelectrolyte chains (as described by the persistence length) is significantly lower than predicted by Odijk−Skolnick−Fixman (OSF) theory. Furthermore, the desorption force of single physisorbed polymer chains from negatively charged silica surfaces was determined. In addition to the electrostatic interaction between polymer and substrate, which depends linearly on the Debye screening length and the polymer's line charge density, a constant nonelectrostatic contribution to the desorption force was observed.

Introduction

Polyelectrolytes are of central importance in nature; e.g., the conformation as well as the adhesive behavior of proteins is governed to a significant extent by electrostatic interactions.[1,2] Besides, due to their unique adsorption properties at interfaces, synthetic polyelectrolytes[3] are used in numerous industrial applications to precipitate small particles in a variety of processes, such as mineral separation,[4] flocculation,[5] retention,[6] or as strength-enhancing additives in paper production.[7] In this context, the cross-linking of particles by polyelectrolyte bridges is of particular importance.[8] Under certain conditions, the surface charge of a substrate is not only neutralized by polyelectrolyte adsorption but even reversed.[9,10] This effect can be used to stabilize colloidal suspensions[11] or for the buildup of multilayered structures of alternating positively and negatively charged polyelectrolyte layers, each only a few nanometers thick.[12] Finally, adsorbed polyelectrolyte layers can serve as biocompatible, soft cushions on solid substrates which can be used to support, e.g., lipid bilayer membranes.[13,14]

In general, polyelectrolyte adsorption is a complex issue, which has attracted both theoretical and experimental scientists from different areas of research. Despite this tremendous effort, the interplay of intramolecular interactions is not completely understood, as long-range electrostatic interactions have to be considered. This provides a significant complication in the theoretical treatment of polyelectrolytes.[15−21]

A number of recent publications are directed at determining the influence of molecular weight, counterion concentration, and polymer and surface charge densities on the layer thickness, the layer structure, and the interaction forces of adsorbed polyelectrolytes at (charged) surfaces. Various experimental techniques such as X-ray and neutron reflectometry,[14,22] atomic force microscopy (AFM),[23,24] or the surface forces apparatus (SFA)[9,25] have been employed to address these issues.

With the development of new experimental tools allowing piconewton force resolution and angstrøm positioning precision of force sensors, mechanical experiments with single molecules have become possible, which have given new insights into intra- and intermolecular forces.[26−31] Furthermore, by investigating single polymers far away from their maximum-entropy conformation, these experiments have inspired new concepts in polymer physics, which go far beyond the classical models of this field and incorporate conformational transitions, enthalpic deformations, and bond rupture of polymers.[32−34]

In this study, AFM based single molecule force spectroscopy has been used for the investigation of polyvinylamine (PVA) on the single molecule level. The fraction of amino groups in the polymer chains was controlled by synthesis such that polyvinylamines of varied line charge density could be investigated. In one set of experiments, the polymers have been covalently attached to aminoreactive surfaces such as epoxy-silanized glass substrates and AFM tips. This allowed for the detection of the polymers' elastic behavior up to forces in the nanonewton range. In a second set of experiments, the desorption of single PVA chains from solid supports was investigated on physisorbed polymer layers.

Materials and Methods

Materials. The polyvinylamines were synthesized by partial hydrolysis of poly-*N*-vinylformamide, such that the fraction of amino groups in the polymer chains could be controlled by

[†] Ludwig-Maximilians Universität.
[‡] BASF-AG.
* Corresponding author: E-mail markus.seitz@physik.uni-muenchen.de.

10.1021/ma0009404 CCC: $20.00
Published on Web 01/12/2001

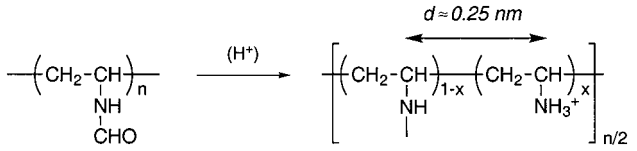

PVA(10%):	x = 0.10,	a = 2.50 nm,	τ = 0.40 nm^{-1}
PVA(30%):	x = 0.32,	a = 0,79 nm,	τ = 1.26 nm^{-1}
PVA(50%):	x = 0.52,	a = 0.48 nm,	τ = 2.08 nm^{-1}
PVA(70%):	x = 0.73,	a = 0.34 nm,	τ = 2.94 nm^{-1}

Figure 1. Molecular structure of polyvinylamines used in AFM single molecule experiments. x = degree of hydrolysis (i.e., amount/fraction of free amino functions); a = distance between neighboring positive charges as estimated from CPK models; τ = line charge density.

synthesis. In Figure 1, the molecular structure of the PVA polymers, their degree of hydrolysis, x, as determined by stoichiometric control (and checked by NMR), and the line charge density, τ, as estimated from Corey−Pauling−Koltun (CPK) models are shown. The average molecular weight of the polymers as determined by light scattering was $M_w \approx 500\,000$ g mol^{-1} (i.e., the weight-averaged degree of polymerization is $N_w \approx 12\,000$, which gives an average contour length of the polymers, $L_{avg} \approx 3\,\mu$m). (3-Glycidyloxypropyl)trimethoxysilane was purchased from Aldrich (Deisenhofen, Germany); all other solvents and sodium chloride were purchased from Sigma (Deisenhofen, Germany). Deionized water was further purified using a Milli-Q plus system (σ = 18.2 MΩ·cm, π = 71 mN/m).

Surface Functionalization of Glass Substrates and AFM Tips (Figure 2). Glass microscope slides (25 × 75 × 1 mm, Sigma) as well as silicon substrates with native oxide layers (Wacker, Germany) were cleaned prior to the experiment by sonicating for 10 min in Hellmanex solution (Hellma, Mühlheim, Germany) and twice in Milli-Q water.

The cleaned SiO_x substrates were functionalized in a 5 vol % solution of (3-glycidyloxypropyl)trimethoxysilane in 2-propanol for 1 h. The substrates were then kept in an oven at 80 °C for 3 h, followed by successive rinsing with 2-propanol. Increased hydrophobicity of the substrates was observed in contact angle measurements after silanization. Si_3N_4 AFM tips were used as obtained from Microlevers, Park Scientific Instruments, Sunnyvale, CA, and epoxy-functionalized by the same silanization procedure.

Polyvinylamine was attached to the substrates by incubating a small region of the surface with a few drops of an aqueous polymer solution (0.2 mg mL^{-1}) for 30 min, followed by successive rinsing with Milli-Q water. This procedure allows for both physisorption of the polymers onto the negatively charged glass substrate and covalent binding of the amino groups to epoxy-functionalized supports (as shown by the high rupture forces in the elasticity experiments).

AFM Experiments. The samples were then mounted in a custom-built AFM with a z range of the piezo translator of 15 μm. Details of the experimental setup are given elsewhere.[35,36] All experiments were conducted in solutions of 1:1 electrolytes (NaCl) at room temperature (21 °C), unless otherwise specified.

For the characterization of elastic properties, the epoxy-functionalized AFM tip was brought in contact with an interfacial layer of covalently bound PVA molecules on glass (microscope) slides by manual control. The AFM tip and the polymer layer were kept in contact under a contact force of several nanonewtons (nN) for approximately 30 s, which is sufficient to allow for a chemical reaction between the epoxy functions at the tip surface and the amino groups of the polymer. Upon retraction of the cantilever, individual PVA molecules were stretched between two covalent links of the polymer to the surface and the AFM tip (Figure 3a). The resulting forces profiles were measured via the deflection of the AFM cantilever spring using optical lever detection.[37] The

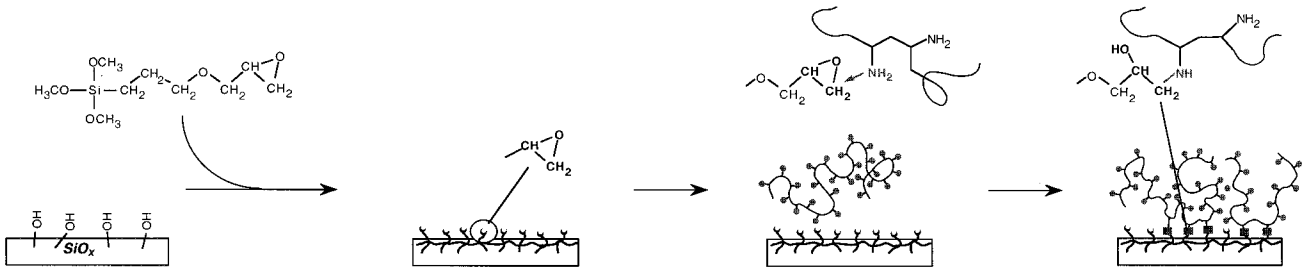

Figure 2. Covalent attachment of polyvinylamine to epoxy-funtionalized surfaces. Surface hydroxy functions (naturally present on silica substrates as well as on silicon nitride AFM tips) are converted to amino-reactive epoxy functions via silanization. Chemical reaction with amino functions of PVA yields β-hydroxyalkylamine function.

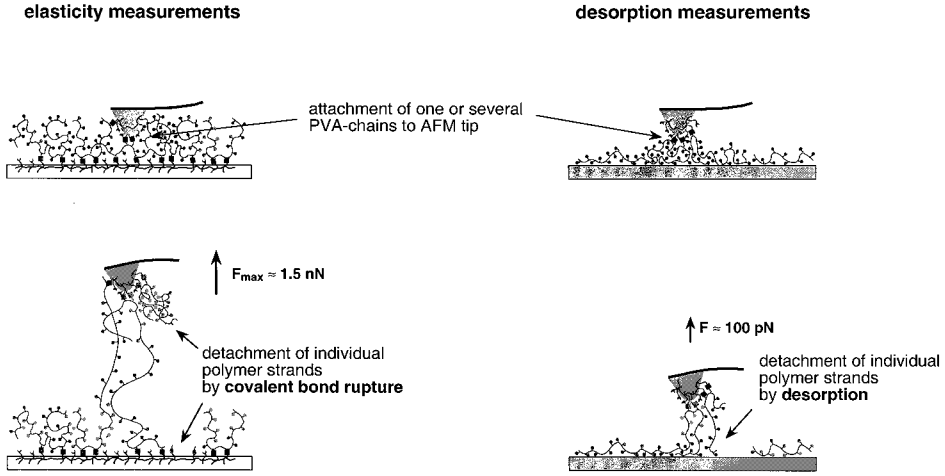

Figure 3. Comparison of elasticity and desorption experiments. In the elasticity experiment, the polymer is covalently fixed to both substrate and AFM tip; in the desorption experiment, PVA is physisorbed to the substrate and only covalently attached to the AFM tip. Detachment in elasticity experiments occurs when a covalent bond ruptures along the stretched polymer strand (nanonewton forces); in desorption experiments ionic bonds between substrate and polymer break under forces in the piconewton range.

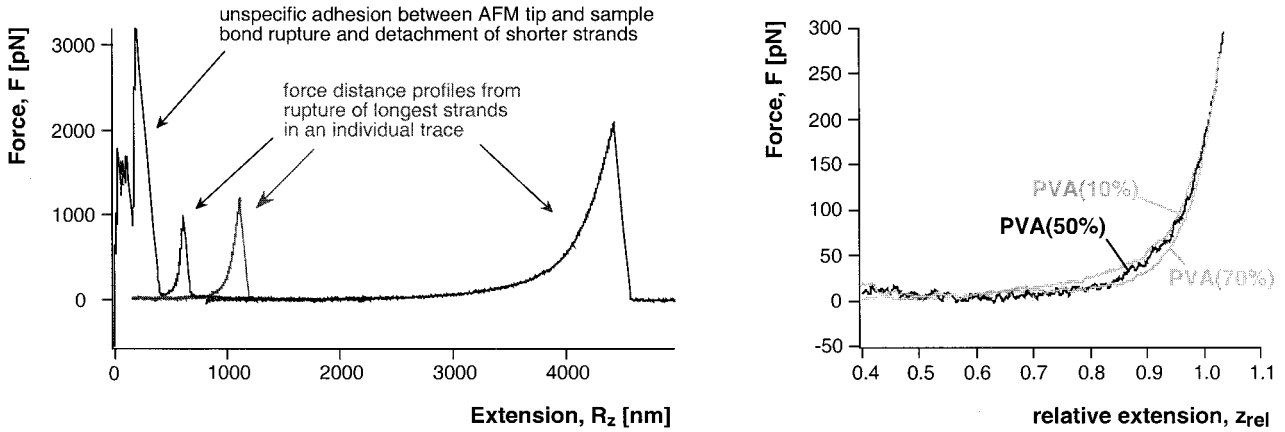

Figure 4. (a) Elastic behavior of PVA(50%) covalently fixed between glass substrate and AFM tip. Three typical traces of individual strands of different contour length are shown. At short distances, the profiles are dominated by a strong adhesive force which is illustrated in one of the curves (but has been omitted for clarity of presentation in the other three traces). For identification of single polymer traces and for comparison of different PVA samples, the measured curves are normalized and superimposed; here, $z_{rel} = 1.0$ for $F = 200$ pN was chosen. The normalized curve for PVA(50%) is plotted in (b) and compared with the force−distance profiles of polyvinylamines of different degree of hydrolysis (line charge density), PVA(10%) and PVA(70%); all shown curves were measured in 5 mM NaCl solution.

nominal spring constants of cantilevers used in the experiments were 10 or 30 mN/m. Prior to the first approach of the AFM tip to the surface, the spring constants of each lever were individually calibrated by measuring the amplitude of its thermal oscillations.[38] The sensitivity of the optical lever detection was measured by indenting the AFM tip into a hard surface.

Note that, as indicated in Figure 4, the first force−distance profile recorded after tip−substrate contact can be rather complex, consisting of contributions from stretching several polymer strands, desorption of the polymer strands from substrate and/or cantilever, covalent bond rupture of short strands, and interchain aggregation and entanglements. Therefore, in each measurement the cantilever was first retracted from the substrate to a distance at which unspecific adhesion was no longer observed. Then, in successive retraction−approaching cycles the distance range is increased while avoiding contact between the tip and additional PVA strands at the substrate surface, until only one polymer strand remained between tip and substrate. The force−distance profile of this strand was then measured repeatedly until rupture.

Assuming that in the probed force regime the measured stretching force is a function of the relative extension of the polymer chain, i.e., $F \sim f(R_z/L)$, all force traces originating from single polymer chains should superimpose when scaled to the same contour length. In turn, the superposition of the force traces serves as an additional criterion for the identification of single polymer strands.[29,35] Here, for comparison of the force profiles measured on PVA strands of different lengths, the relative extension z_{rel} in all traces was set to $z_{rel} = 1$ at a force of 200 pN.

For the desorption experiments, PVA was physisorbed onto unfunctionalized glass substrates from aqueous solution under the same experimental conditions as given above. Again, epoxy-functionalized tips were employed to covalently bind the amino groups of the polymer in the AFM experiment. As indicated in Figure 3b, the weakest links in this system are the ionic bonds between polymer and substrate. Therefore, the resulting force profiles are determined by the detachment of the polyelectrolyte chains from the substrate at forces of several hundred piconewtons while the covalent link to the AFM tip holds forces up to the nanonewton range.[30] In this case, contact between tip and substrate was established for several seconds in each cycle followed by retraction of the tip until no more adhesive force was detected.

Results

Mechanical Properties of Single Polyvinylamine Molecules. Figure 4a shows various experimental force−distance traces of individual PVA(50%) strands of different length in 5 mM NaCl solution at room temperature. The covalent attachment of the polymer to both substrate and AFM tip allows for the elastic characterization of the polymers up to nanonewton forces.[39]

The elasticity of polyelectrolytes is expected to depend on the distance of electrical charges (i.e., ionic or ionizable funtional groups) along the polymer chain as well as on the screening of these charges in electrolyte buffers.[15,18] Therefore, force−extension curves of polyvinylamine were determined at varied charge density of the polymer and at different salt concentrations of the buffer solution. Figure 4b shows normalized curves for three different polyvinylamines, all measured in 5 mM NaCl solution. Qualitatively, the change in curvature of the force−distance profiles already indicates the expected effect: increasing the polymer's line charge density increases its bending rigidity. Likewise, a change in electrolyte concentration was found to affect the bending rigidity of PVA, while the influence of pH change was negligible in the investigated range from pH 5 to 9 (i.e., below the estimated pK_b of the polymers and above the pK_a of the silica substrate).

For quantitative comparison of the experimental data with theoretical predictions for polyelectrolyte elasticity, the experimental curves were fitted by an extended wormlike chain (WLC) model including linear elastic contributions arising from the stretching of bond angles and covalent bonds.[40]

$$F\frac{L_p}{k_B T} = \frac{R_z}{L} - \frac{F}{K_0} + \frac{1}{4(1 - R_z/L + F/K_0)^2} - \frac{1}{4} \quad (1)$$

In this expression, R_z is the measured end−end distance at any given force, F, and L is the contour length of the stretched chain (polymer strand) under zero force ($F = 0$). The polymer's bending rigidity is expressed by the chain's persistence length, L_p. Finally, the chain's extensibility upon stretching is described by the segment elasticity, K_0, which is introduced into eq 1 as a linear term. (Hereby, K_0 can be understood as the inverse of the normalized compliance of a Hookean spring; the spring constant of the polymer chain is given by K_0/L.) Note that eq 1 is only based on an approxima-

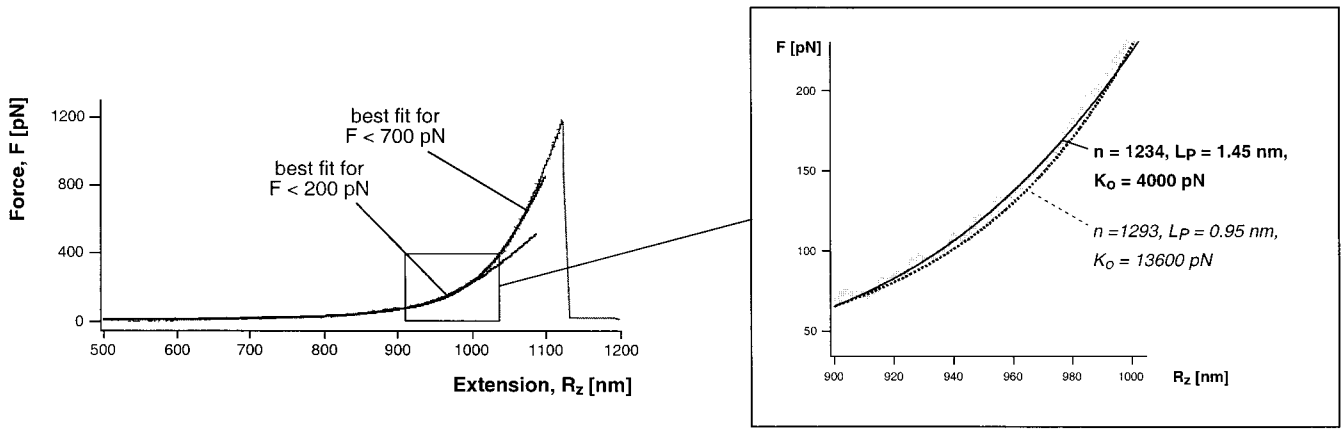

Figure 5. WLC fits to force−distance profile obtained for PVA(50%) in 5 mM NaCl solution: (a) two fit curves to experimental trace for $F \leq 200$ pN and $F \leq 700$ pN; (b) a close look at the curvature of experimental and fitted curves shows the different quality of the fits and the dependence of the fit parameters upon the choice of the force range (gray, experimental trace; black line, fit to $F \leq 200$ pN; dotted line, fit to $F \leq 700$ pN).

tion to the exact solution of the WLC model. This approximation is valid in the range of very low and high forces (i.e., in the regimes $F < 1$ pN and $F > 20$ pN).[41] At forces above 200 pN, nonlinear contributions to the extensibility of the molecule are likely to become important such that the description of the enthalpic stretching by a simple Hooke spring may no longer be a good approximation which is illustrated in Figure 5.

For the evaluation of the PVA elasticity data, only such force−distance curves were considered which perfectly superimposed within the experimental noise. One of these superimposed curves was chosen for the fitting of the experimental curves according to the extended WLC model given by eq 1. Two fit curves are shown which model the experimental force−distance profile of PVA(50%) in 5 mM NaCl solution in the range of $F < 200$ pN (solid line) and $F < 700$ pN (dashed line). The fit curves were obtained by minimizing the mean standard deviation, $\sigma^2 = \sum(F_{exp} - F_{fit})^2/N^2$, of the fit, resulting in $\sigma = 0.022$ and $\sigma = 0.035$, respectively. However, to allow for a reasonable statistical comparison of the two fits, the standard deviations were compared only for the range of $F < 200$ pN which, for the fit up to 700 pN, gave $\sigma = 0.024$ for force values, $F < 200$ pN. While this difference in the standard deviation between the two fits may appear only marginal, there is a significant deviation in the fit results obtained for the different regimes. For the best fit curve in the range of $F < 200$ pN, a persistence length of $L_p = 1.45$ nm was calculated which is almost twice as high as the value obtained for the best fit over the larger force range ($F < 700$ pN, $L_p = 0.95$ nm). Also, a higher stiffness of the polymer chain is indicated by a higher segment elasticity, $K_0 = 13\,600$ pN at high forces, as compared to $K_0 = 4000$ pN when only the lower force range is considered. A close look at the curves in the regime between $F = 100-200$ pN also reveals that the experimental data are modeled with a significantly better accuracy by the solid line, i.e., the fit curve for the low force range. Moreover, the fit parameters are consistent and independent of the force range as long as $F < 200$ pN; i.e., a further decrease of the fitted force range did not affect the resulting values for L_p and K_0.

Thus, to extract the persistence length, L_p, from the experimental data, for each fit the force range was decreased until a constant value was obtained. Note, however, that a vertical force offset of ±1 pN results in a ~10% deviation of the calculated persistence length. Considering the experimental noise at forces below 20 pN, a relative error of $\Delta L_p \approx 20\%$ is therefore estimated. The value of the segment elasticity is even more affected by the experimental accuracy in determining zero force and zero extension. Thus, data for K_0 can be given within a relative experimental error of $\Delta K_0 \approx 50\%$. The elasticity data for polyvinylamines of different charge density measured at different salt concentration are given in Table 1.

Table 1. Persistence Length, L_p, and Segment Elasticity, K_0, of Polyvinylamines with Different Degrees of Hydrolysis (Line Charge Density, τ), Measured under Conditions of Varied Salt Concentration As Obtained from WLC Fits to the Experimental Force−Distance Profiles; Estimated Relative Experimental Errors Are $\Delta L_p \approx 20\%$, and $\Delta K_0 \approx 50\%$

polymer	c_{salt} [mM]	L_p [nm]	K_0 [pN]
PVA(10%)	5	0.8	5100
	10	0.9	4100
	100	0.95	3600
PVA(30%)	5	0.45	4800
	10	0.85	4500
	40	1.0	3000
	100	0.9	3700
PVA(50%)	5	1.45	4000
	10	1.75	4500
	40	1.65	5000
	100	0.85	4000
PVA(70%)	5	2.0	5200
	10	1.2	5700
	100	1.2	6500

Desorption of Polyvinylamine Chains from Solid Substrates. In addition to studying the elastic behavior of single polymer chains discussed in the previous section, single molecule force spectroscopy can also be used to probe the adhesion forces of physisorbed polyelectrolyte chains on solid substrates. Again, epoxy-functionalized AFM tips were used to allow for a covalent binding of polyvinylamine as the tip was brought in contact with the interfacial polymer layer. Then, upon retracting the cantilever, the resulting forces were measured as one or more polymer strands were covalently grafted to the tip and successively pulled off the substrate. Figure 6 shows two representative curves of polyvinylamine desorption from bare glass substrates.

A force−distance trace recorded upon detachment of a single polyvinylamine chain from silica (here, PVA(70%)

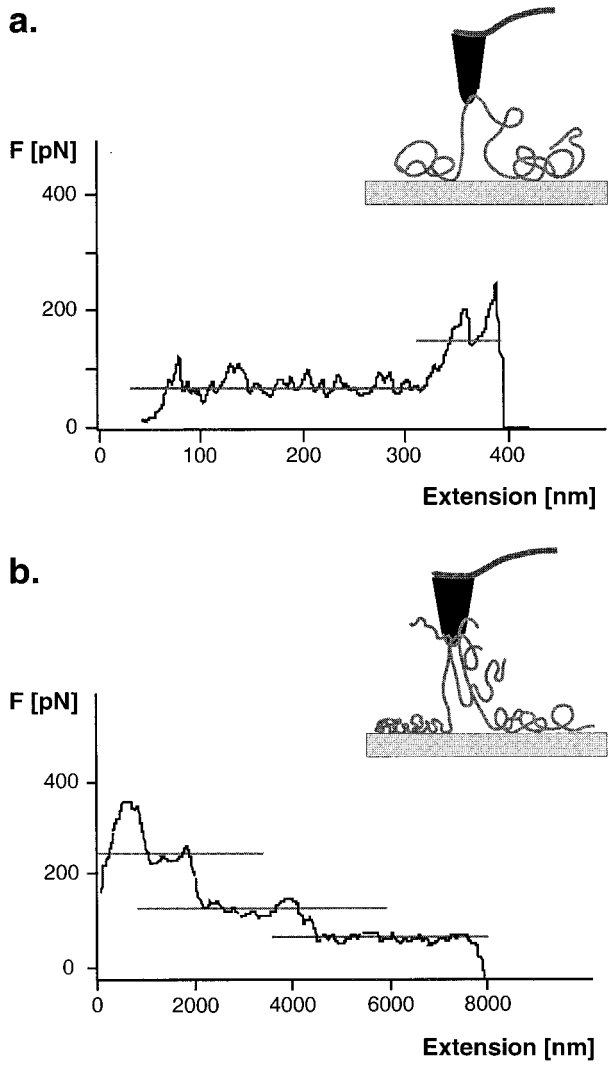

Figure 6. Typical force−distance profiles measured upon detachment of physisorbed polyvinylamines from a charged surface: (a) stretching and desorption of a single loop; (b) stretching and desorption of multiple strands.

measured in 5 mM NaCl solution) is shown in Figure 6a. In some cases, one loop of the polymer chain is picked up upon covalent attachment to the AFM tip at a random position, such that its two strands bridging between substrate and tip are of different length. While retracting the cantilever, the shorter strand is stretched which gives rise to the characteristic stretching trace at low forces until a plateau region of constant force ($F \approx 50-100$ pN) is observed.

Recent theoretical considerations by Haupt et al.[42] have suggested that the shape of the force−extension profile for the continuous desorption of a weakly adsorbed polymer chain from a solid substrate depends on the force loading rate. While at fast pulling rates each monomer−surface detachment provides a peak of a sawtooth pattern, the height of the individual peaks related to the consecutive dissociation events is reduced with decreasing pulling rates, effectively resulting in a flat plateau of constant force at infinitely slow pulling rate. Hereby, an important parameter determining the peak height is the natural off-rate of the monomer−surface contacts. In the experiments described here, the dissociation of ionic bonds between individual amino groups and charged surface sites can be expected to be much faster than the applicable force loading rates.

Thus, each observed plateau region can be interpreted as the continuous desorption of one ore several polyelectrolyte strands. In Figure 6a, both ends of the loop are being stretched and desorbed simultaneously from the substrate as the length of the stretched (initially shorter) strand becomes comparable in size to the other strand of the loop. As a result, the required desorption force doubles, as indicated in the recorded trace by a stepwise increase followed by a second plateau region at twice the height of the first plateau. Finally, full desorption of both ends results in rupture of the system and the recorded (adhesive) force drops to zero.[43]

However, the stretching and desorption of a single loop was only the simplest case observed. Figure 6b shows a force curve which was found for the desorption of multiple molecules (loops). At short distances, a steep increase of the force resulting from the simultaneous stretching of several polymer strands is recorded. As the distance between tip and substrate is increased, their continuous desorption is again indicated by a plateau of constant force. As the shortest PVA strand fully detaches from the substrate, a decreasing step in the force profile is measured, followed by the successive detachment of all polymer chains, each reflected by a stepwise decrease in the overall desorption force. As in the elasticity experiments, the contour lengths of the desorbed polyvinylamine chains varied between 0.5 and 8 μm. (Considering the broad molecular weight distribution of the materials, this is in accordance with the estimated average polymer chain length of 3 μm.)

Although most of the recorded traces were more complex than the two most illustrative examples shown in Figure 6, in all cases the typical plateaus of constant force were observed. In accordance with the discussion of the underlying molecular processes given above, the step heights were thus interpreted as the contribution of individual PVA strands to the overall recorded desorption forces. Although the simultaneous detachment of two or even three strands was occasionally observed, most of the steps indeed originated from single PVA strands. In the following, we will thus refer to the plateau steps as desorption forces.

The desorption forces for differently substituted polyvinylamines from silica substrates are summarized in Figure 7. In the histograms, the force distributions determined from experimental series under varied conditions of polymer charge density and salt concentration are plotted.

The gray bars represent those step heights which have been interpreted as multiple chain desorption events. They were neglected for the determination of the average values. As expected, a decrease in polymer charge density as given in PVA(50%), PVA(30%), and PVA(10%) resulted in smaller average desorption forces (Figure 7a). As in the elasticity measurements, no significant pH dependence in the range from pH 5−9 was observed.

In solutions of high electrolyte concentration (100 mM), i.e., under efficient screening conditions of the electrostatic surface potential (Debye length, $\kappa^{-1} \approx 0.95$ nm),[44] the desorption forces of PVA(70%) are decreased to an average value of ~45 pN, which is in the same range as for PVA(10%) under similar conditions (Figure 7b). In general, this value gives a lower limit for all investigated polyvinylamines. Presumably, it can be associated with a nonelectrostatic contribution for the measured desorption forces from SiO_x surfaces.

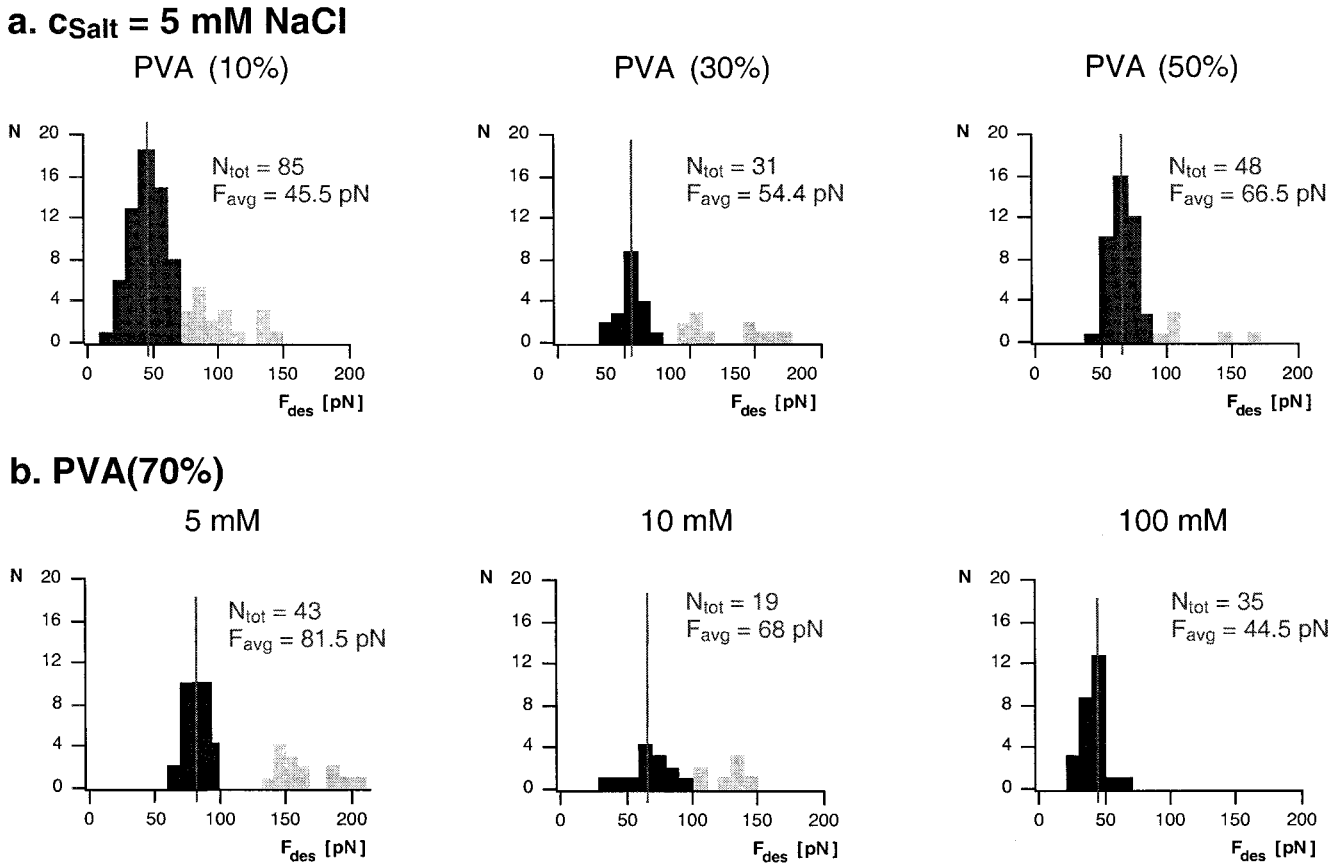

Figure 7. Histograms of desorption forces of polyvinylamine from silica substrates: (a) dependence on polymer charge density (all profiles measured in 5 mM NaCl solution); (b) dependence on salt concentration. Note that, due to thermal noise, the accuracy in determining the average desorption force is limited to a range of ±5 pN; a bin width of 10 pN was chosen in the histograms.

Discussion

Elastic Behavior of Polyvinylamines. From classical Odijk−Skolnick−Fixman (OSF) theory,[15,16] it is expected that the electrostatic interaction between the charges along the polyelectrolyte chain increases its bending rigidity: as the repulsive interaction tends to increase the distance between like-charged segments, it favors the stretched conformation of the chains and thus effectively increases the persistence length, L_p, of the molecules by an additional electrostatic contribution, L_{el}. In the rod limit, the electrostatic contribution adds to the purely elastic term, L_0, and is given by

$$L_{el} = l_B \kappa^{-2} \tau^2/4 \qquad (2)$$

where l_B is the Bjerrum length (given by $l_B = e^2/(4\epsilon\epsilon_0 k_B T) = 0.71$ nm in water at room temperature), κ^{-1} is the Debye length which describes the screening of the electrostatic potential in electrolyte solution, and τ is the line charge density of the polyelectrolyte (given by the inverse of the average distance between two charges along the chain; cf. Figure 1). However, at high charge densities, there is a limit for the line charge density as counterion condensation reduces the average distance, a, between two charges along the chain to the Bjerrum length (which defines the distance at which the repulsive interaction of two like charges equals $k_B T$).[45] In this "Manning" limit, the effective line charge density becomes one charge per Bjerrum length, $\tau = l_B^{-1}$, and eq 2 reduces to

$$L_{el} = \kappa^{-2}/4 l_B \qquad (3)$$

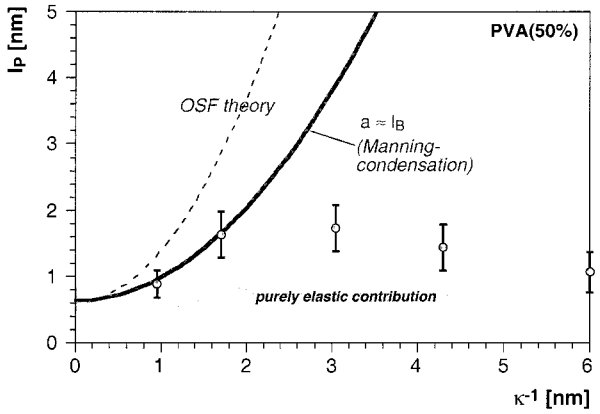

Figure 8. Dependence of the persistence length of PVA(50%) (as obtained from WLC fits) on Debye screening length (cf. Table 1 for other polyvinylamines). Theoretical predictions according to OSF theory are shown as dotted and solid curves. The solid curve corresponds to the "Manning limit" considering counterion condensation ($a \approx l_B$).

In Figure 8, the persistence lengths obtained for PVA(50%) from the WLC fit of the experimental force−distance profiles are plotted against the Debye length, κ^{-1}, of the buffer solution (also compare Figure 4b and Table 1). Assuming a purely elastic persistence length of $L_0 = 0.8$ nm (as measured for the nearly uncharged PVA(10%) under high screening conditions), the comparison with the theoretical curves from OSF theory shows that the observed electrostatic contribution, L_{el}, is much less than expected, especially at conditions of low salt concentration (i.e., for large κ^{-1} or little screening of the electrostatic interactions).

This is in qualitative agreement with early measurements on the salt dependence of DNA elasticity by Smith et al. using magnetic beads,[28] as well as with recent observations on synthetic polyelectrolytes employing the AFM technique.[31,46] However, a quantitative comparison of experimental data on the different synthetic polyelectrolytes is not straightforward as the reported data are based on different fit models. As already discussed above, the introduction of (linear) elastic stretching terms into the WLC model (eq 1)[34,40,47] as well as the choice of the lower force regime for fitting has the effect of yielding increased values for the polymers' persistence lengths. Moreover, an improved theoretical description of the measured force−distance profiles at high forces is expected from the consideration of cross-terms obtained from coupling the bending and stretching fluctuations, together with the introduction of nonlinear elastic contributions to the polymer extensibility.[48]

Despite the uncertainties related to the fitting process itself, they are by no means sufficient to explain the drastic difference between the theoretical predictions from OSF theory and the experimental data. However, it has to be recognized that the OSF theory considers the electrostatic contribution only based on a static approach. Considering dynamic bending fluctuations along the polyelectrolyte chain, it has been shown already by Barrat and Joanny[19] that the electrostatic contribution to the chain stiffness, described by L_{el}, depends on the scale of the bending fluctuations. For bending wavelengths smaller than the Debye screening length, κ^{-1}, the persistence length of the charged chain is effectively reduced to the bare elastic contribution. Marko and Siggia[32] recognized that this results in an apparent reduction of the effective bending stiffness upon stretching, which could explain the observed salt and force dependence of DNA bending rigidity.[28] A universal scaling function for the force dependence of the electrostatic persistence length, L_{el}, has been given recently by Netz.[48] Hereby, it has been suggested that the crossover from a "lower force regime", in which the electrostatic contribution, L_{el}, efficiently increases the persistence length of the polymer, to a "higher force regime", in which the bending elasticity is given by the bare elastic contribution L_0, depends on L_0 as well as on the Debye screening length, κ^{-1}. At comparable salt concentration an efficient softening of synthetic polyelectolyte chains ($L_0 \approx 1$ nm) should thus occur already at forces 1 order of magnitude smaller than for DNA ($L_0 \approx 30$ nm).[48] At forces of 10 pN and under conditions of low screening, DNA can therefore be described by a semiflexible chain with a persistence length of $L_p \approx 50$ nm, which corresponds to the sum of the bare elastic and the electrostatic persistence length,[28,32] while the polyvinylamines investigated in our work are described by a persistence length corresponding to the bare persistence length, $L_p \approx L_0 \approx 1$ nm.

As indicated above, a decrease of the Debye screening length can result in a crossover from the "high force regime" to the "low force regime". This is seen in Figure 8 in which a maximum value for the persistence length is observed for $\kappa^{-1} \approx 2.3$ nm. Apparently, at this crossover point the bending wavelengths of the PVA(50%) chain become comparable to the Debye screening length.

Desorption Forces of Polyvinylamines from Silica Substrates. As indicated above, the dissociation rate of ionic bonds between the positively charged amino groups of the polymer and the negatively charged surface sites is much faster than the pulling rate applied in our experiments. Thus, on the time scale of the experiment, the polyelectrolyte chain can be considered as a string of constant charge continuously desorbing from the charged substrate against the attractive potential of the surface. The electrostatic contribution to the force that needs to be applied in order to induce this continuous desorption can be quantified as follows. The electrostatic potential, $V^{el}(z)$, of the substrate in electrolyte buffer is given in the Debye−Hückel approximation by

$$V^{el}(z)/k_BT = 4\pi l_B \sigma \kappa^{-1} \exp(-\kappa z) \qquad (4)$$

in which σ is the surface charge density.[44] Upon desorption of one polymer segment of length a, the entire polymer chain is moved against the electrostatic surface potential; i.e., the separation of each charged segment from the substrate is increased by the distance a. Therefore, the force that needs to be applied for this process can be determined simply from the transfer of one charged segment from $z = 0$ to $z = \infty$ while all other segments stay in place (Figure 9a). It is obtained as

$$F_{des}^{el} = (4\pi l_B k_B T)\sigma \kappa^{-1} \tau \qquad (5)$$

Thus, at constant surface charge density, a linear dependence of the desorption force on the Debye length, κ^{-1} (for constant polymer charge), as well as on the line charge density, τ (for constant electrolyte concentration), is expected. The data obtained for the desorption of PVA from silica substrates are plotted in Figure 9b (F_{des} vs κ^{-1}) and Figure 9c (F_{des} vs τ), and their dependence on the given parameters is as predicted.

As shown for PVA(30%) and PVA(70%), a linear increase in the desorption force is found with increasing Debye length resulting from the electrostatic interaction between polymer and substrate. By extrapolation to $\kappa^{-1} = 0$, $F_0 \approx 33$ pN is obtained, which can be considered a "zero charge" contribution to the desorption force of PVA chains from silica. It is independent of electrostatic charges and most likely dominated by van der Waals interactions between polymer and substrate.[49] In a first approximation, the electrostatic force, F_{el} (eq 5), is therefore supposed to be the only additive term to the overall desorption force, F_{des}, such that

$$F_{des} = F_0 + (4\pi l_B k_B T \sigma)\kappa^{-1} \tau \qquad (6)$$

Thus, the surface charge density, σ_{SiOx}, of the silica substrates used in the experiments can be extracted from the slopes of the line fits for the two different polymers shown in Figure 9b. On the basis of the estimated line charge densities of the polymers (cf. Figure 1), $\sigma_{SiOx} = 0.131$ nm^{-2} (i.e., 0.022 C m^{-2}) and $\sigma_{SiOx} = 0.103$ nm^{-2} (i.e., 0.017 C m^{-2}) are obtained for PVA(30%) and PVA(70%), respectively, which is in good agreement with values reported in the literature.[44,50] The maximum surface charge densities for uncoated silica surfaces lie in the range of $\sigma_{SiOx} \approx 0.4$ C m^{-2},[51] but it has to be considered that this value is significantly reduced in electrolyte solutions.[44]

In Figure 9c, the experimental data for different PVA samples in 5 mM NaCl solution are plotted against the charge density of the polymers. Again, the expected increase in the average desorption force is observed, and

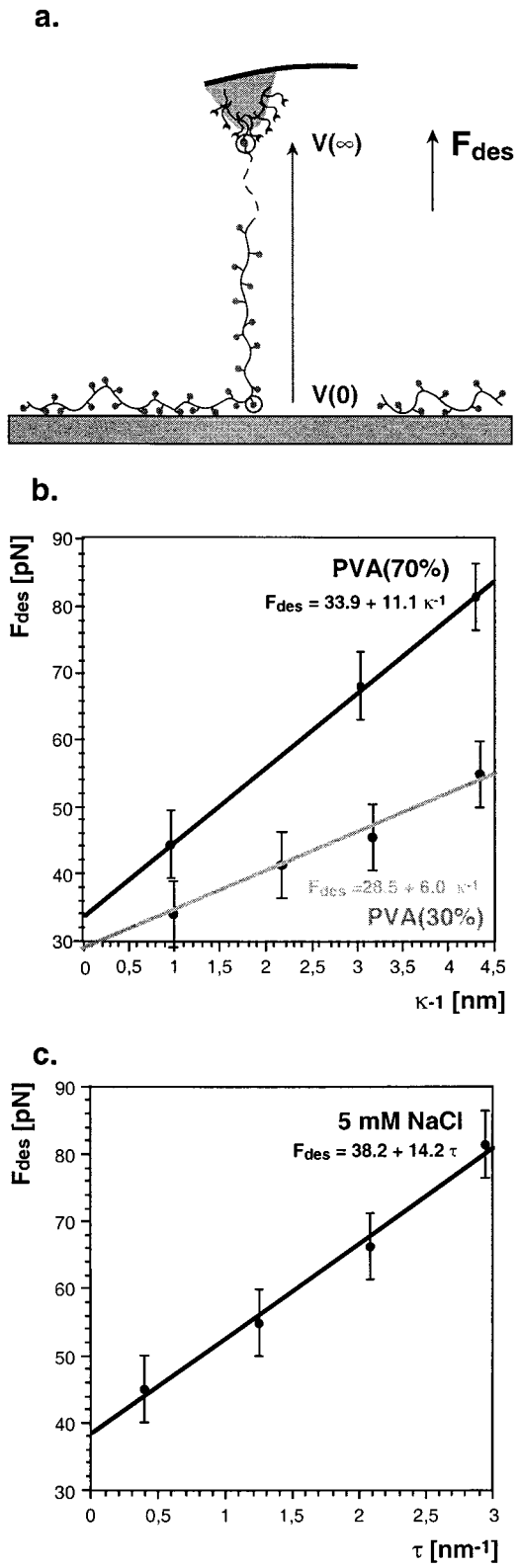

Figure 9. (a) Continuous desorption of charged polymer chains from a charged substrate. (b) Dependence of desorption force on Debye screening length plotted for PVA(30%) and PVA(70%). (c) Dependence of desorption force on polymer line charge density measured in 5 mM NaCl solution ($\kappa^{-1} \approx 4.3$ nm).

the data have been fitted by a straight line according to eq 6. Here, the surface charge density of the silica substrate is determined as $\sigma_{SiOx} = 0.091$ nm^{-2} (i.e., 0.015 C m^{-2}), which corresponds within the experimental error to the value obtained from Figure 9b. Also, the zero charge contribution $F_0 \approx 38$ pN from this fit is in agreement with the constant term of the desorption force calculated above, which again indicates its non-electrostatic origin. Finally, the surface potential, ψ_0 ($\approx V(0)$), of the substrate is obtained from eq 4 and eq 6 as $(F_{des} - F_0) = V(0)\tau = \psi_0\tau$, i.e.

$$\psi_0 = F_{el}/\tau \tag{7}$$

According to our simple model, the surface potential of the silica substrate is thus given by the slope of the linear fit to the experimental data in Figure 9c, such that ψ_0(silica) $= -14.2$ pN nm (unit charge)$^{-1} \approx -88$ mV. Although this value is slightly higher than expected,[23,44,50] it still indicates that the simple linear model used here is a good first approximation and well-suited to explain the observed desorption forces of polyelectrolytes from charged substrates.

Conclusions

Single polyvinylamine chains of varied line charge density have been investigated using AFM based single molecule force spectroscopy. It has been shown that the electrostatic contribution to polyelectrolyte elasticity, which is known to effectively increase the persistence length of the polymers at zero load, vanishes under high mechanical stresses. On the basis of these findings, an improved theoretical understanding of polyelectrolyte elasticity at high forces should emerge. Furthermore, the detachment force of single polyvinylamine chains from silicon oxide surfaces has been determined as a function of polymer line charge density as well as electrolyte concentration. Within the experimental errors, the results could be described by a simple linear model with a linear dependence of the detachment force on the polymer line charge density as well as the Debye screening length. On the basis of this model, the surface charge density as well as the surface potential of the silica substrate could be deduced from the experimental data. In addition to the electrostatic contribution, a constant detachment force presumably due to the non-electrostatic interaction between polymer and substrate surface was found. Single molecule force spectroscopy by AFM thus allows to measure adhesive forces on the single molecule level and to gain detailed insight into fundamental interactions in colloidal systems.

Acknowledgment. The authors acknowledge the technical help of Patrick Schulz-Vanheyden and Alexander Schemmel (Lehrstuhl für Angewandte Physik, LMU München). We also thank Roland Netz (MPI Kolloidforschung, Golm) for helpful discussions and Norbert Mahr (BASF AG, ZDH) for providing the PVA samples. The work was financially supported by the Deutsche Forschungsgemeinschaft (DFG) and the Fonds der Chemischen Industrie.

References and Notes

(1) Kyte, J. *Structure in Protein Chemistry*; Garland Publishing: New York, 1995.
(2) Ratner, B. D.; Hoffman, A. S.; Schoen, F. J.; Lemons, J. E. *Biomaterials Science*; Academic Press: San Diego, 1996.
(3) Dautzenberg, H.; Jaeger, W.; Kötz, J.; Philipp, B.; Seidel, C.; Stscherbina, D. *Polyelectrolytes—Formation, Characterization and Application*; Hauser Publications: Munich, 1994.
(4) Hesselink, T. T. *J. Colloid Interface Sci.* **1977**, *60*, 448−465.
(5) Fleer, G. J.; Lyklema, J. *J. Colloid Interface Sci.* **1974**, *167*, 228. (b) Matsumoto, T.; Adachi, Y. *J. Colloid Interface Sci.* **1998**, *204*, 328−335.

(6) Horn, D., Linkart, F., Roberts, Ed.; Blackie Academic & Professional: Glasgow, 1996; pp 64−82.
(7) Wagberg, L.; Kolar, K. *Ber. Bunsen-Ges. Phys. Chem.* **1996**, *100*, 984−993.
(8) Hunter, R. J. *Foundations of Colloid Science*; Oxford University Press: Oxford, 1991.
(9) (a) Dahlgren, M. A. G.; Claesson, P. M. *Prog. Colloid Polym. Sci.* **1993**, *93*, 206−208. (b) Dahlgren, M. A. G.; Claesson, P. M.; Audebert, R. *J. Colloid Interface Sci.* **1994**, *166*, 343−349.
(10) Netz, R. R.; Joanny, J.-F. *Macromolecules* **1999**, *32*, 9013−9025.
(11) Klein, J.; Luckham, P. F. *Colloids Surf.* **1984**, *10*, 65−76.
(12) (a) Decher, G.; Hong, J. D. *Macromol. Chem. Macromol. Symp.* **1991**, *46*, 321. (b) Decher, G. *Science* **1997**, *277*, 1232−1237 and references herein.
(13) Lindholm-Sethson, B. *Langmuir* **1996**, *12*, 3305−3314.
(14) Wong, J. Y.; Majewski, J.; Seitz, M.; Park, C. K.; Israelachvili, J. N.; Smith, G. S. *Biophys. J.* **1999**, *77*, 1445−1457.
(15) Odijk, T. *J. Polym. Sci.* **1977**, *15*, 477−483.
(16) Skolnick, J.; Fixman, M. *Macromolecules* **1977**, *10*, 944−948.
(17) Odijk, T. *Macromolecules* **1977**, *12*, 688−693.
(18) Odijk, T.; Houwaart, A. C. *J. Polym. Sci., Polym. Phys. Ed.* **1978**, *16*, 627−639.
(19) Barrat, J. L.; Joanny, J. F. *Europhys. Lett.* **1993**, *24*, 333−338.
(20) Netz, R. R.; Orland, H. *Eur. Phys. J. B* **1999**, *8*, 81−98.
(21) Châtellier, X.; Joanny, J.-F. *Phys. Rev. E* **1998**, *57*, 6923−6935.
(22) (a) Schmitt, J.; Grünewald, T.; Kjaer, K.; Pershan, P.; Decher, G.; Lösche, M. *Macromolecules* **1993**, *26*, 7058−7063. (b) Rädler, J.; Koltover, I.; Salditt, T.; Safinya, C. *Science* **1997**, *275*, 810−814. (c) Majewski, J.; Wong, J. Y.; Park, C. K.; Seitz, M.; Israelachvili, J. N.; Smith, G. S. *Biophys. J.* **1998**, *75*, 2363−2367. (d) Plech, A.; Salditt, T.; Munster, C.; Peisl, J. *J. Colloid Interface Sci.* **2000**, *223*, 74−82.
(23) Hartley, P. G.; Scales, P. J. *Langmuir* **1998**, *14*, 6948−6955.
(24) (a) Caruso, F.; Furlong, D. N.; Ariga, K.; Ichinose, I.; Kunitake, T. *Langmuir* **1998**, *14*, 4559−4565. (b) Clausen-Schaumann, H.; Gaub, H. E. *Langmuir* **1999**, *15*, 8246−8251. (c) Kolarik, L.; Furlong, D. N.; Joy, H.; Struijk, C.; Rowe, R. *Langmuir* **1999**, *15*, 8265−8275.
(25) (a) Luckham, P. F.; Klein, J. *J. Chem. Soc., Faraday Trans. 1* **1984**, *80*, 865. (b) Kamiyama, Y.; Israelachvili, J. *Macromolecules* **1992**, *25*, 5081−5088. (c) Parker, J. L. *Prog. Surf. Sci.* **1994**, *47*, 205. (d) Lowack, K.; Helm, C. A. *Macromolecules* **1998**, *31*, 823−833. (e) Abe, T.; Higashi, N.; Niwa, M.; Kurihara, K. *Langmuir* **1999**, *15*, 7725−7731. (f) Poptoshev, E.; Rutland, M. W.; Claesson, P. M. *Langmuir* **1999**, *15*, 7789−7794. (g) Poptoshev, E.; Rutland, M. W.; Claesson, P. M. *Langmuir* **2000**, *16*, 1987−1992.
(26) Binnig, G.; Quate, C. F.; Gerber, C. *Phys. Rev. Lett.* **1986**, *56*, 930−933.
(27) (a) Kuo, S. C.; Sheetz, M. P. *Science* **1993**, *260*, 232−234. (b) Florin, E.-L.; Moy, V. T.; Gaub, H. E. *Science* **1994**, *264*, 415−417. (c) Lee, G. U.; Kidwell, D. A.; Colton, R. J. *Langmuir* **1994**, *10*, 354−357. (d) Merkel, R.; Nassoy, P.; Leung, A.; Ritchie, K.; Evans, E. *Nature* **1999**, *397*, 50−53. (e) Wang, M. D.; Yin, H.; Landick, R.; Gelles, J.; Block, S. M. *Biophys. J.* **1997**, *72*, 1335−1346. (f) Rief, M.; Gautel, M.; Oesterhelt, F.; Fernandez, J. M.; Gaub, H. E. *Science* **1997**, *276*, 1109−1112. (g) Kellermayer, M. S.; Smith, S. B.; Granzier, H. L.; Bustamante, C. *Science* **1997**, *276*, 1112−1116.
(28) Smith, S. B.; Finzi, L.; Bustamante, C. *Science* **1992**, *258*, 1122−1126.
(29) Rief, M.; Oesterhelt, F.; Heymann, B.; Gaub, H. E. *Science* **1997**, *275*, 1295−1298.
(30) Grandbois, M.; Beyer, M.; Rief, M.; Clausen-Schaumann, H.; Gaub, H. E. *Science* **1999**, *283*, 1727−1730.
(31) Châtellier, X.; Senden, T. J.; Joanny, J. F.; di Meglio, J. M. *Europhys. Lett.* **1998**, *41*, 303−308.
(32) Marko, J. F.; Siggia, E. D. *Macromolecules* **1995**, *28*, 8759−8770.
(33) (a) Marszalek, P. E.; Oberhauser, A. F.; Pang, Y. P.; Fernandez, J. M. *Nature* **1998**, *396*, 661−664. (b) Heymann, B.; Grubmüller, B. *Chem. Phys. Lett.* **1999**, *303*, 1−9. (c) Rief, M.; Fernandez, J. M.; Gaub, H. E. *Phys. Rev. Lett.* **1998**, *81*, 4764−4767. (d) Kreuzer, H. J.; Wang, R. L. C.; Grunze, M. *New J. Phys.* **1999**, *1*, 21.1−21.16.
(34) Marko, J. F. *Phys. Rev. E* **1998**, *57*, 2134−2149.
(35) Oesterhelt, F.; Rief, M.; Gaub, H. E. *New J. Phys.* **1999**, *1*, 6.1−6.11.
(36) Clausen-Schaumann, H.; Rief, M.; Tolksdorf, C.; Gaub, H. E. *Biophys. J.* **2000**, *78*.
(37) Amer, N. M.; Meyer, G. *Bull. Am. Phys. Soc.* **1988**, *33*, 319.
(38) Butt, H. J.; Jaschke, M. *Nanotechnology* **1995**, *6*, 1−7.
(39) In earlier studies of covalently attached polymers on silanized glass substrates, the rupture of the Si−C bond in the silane anchor determined the available force range. There, an average rupture force of ∼2 nN was observed (cf. ref 30). Here, the β-hydroxyalkylamino groups formed upon reaction of amino groups with the epoxysurface functions appears to be the limiting factor. On average, the investigated system holds forces of ∼1.3 nN, the highest observed rupture force of single polymer strands was ∼1.9 nN (compare Figure 4a).
(40) Odijk, T. *Macromolecules* **1995**, *28*, 7016−7018.
(41) For comparison, the freely jointed chain (FJC) model has been used but was found to model the experimental data with less accuracy.
(42) Haupt, B.; Ennis, J.; Sevick, E. M. *Langmuir* **1999**, *15*, 3886−3892.
(43) It should be mentioned that usually a readsorption of polyvinylamine molecules was observed when the AFM tip was brought into contact with the surface, following a previously measured desorption profile. For polymers of high charge density such as PVA(70%), occasionally this was even observed on reapproaching the surface before contact between tip and substrate was established.
(44) Israelachvili, J. *Intermolecular and Surface Forces*, 2nd ed.; Academic Press Ltd.: London, 1991.
(45) Manning, G. S. *J. Chem. Phys.* **1969**, *51*, 924.
(46) Ortiz, C.; Hadziioannou, G. *Macromolecules* **1999**, *32*, 780−787.
(47) Bouchiat, C.; Wang, M. D.; Allemand, J.-F.; Strick, T.; Block, S. M.; Croquette, V. *Biophys. J.* **1999**, *76*, 409−413.
(48) Netz, R. R. *Europhys. Lett.*, to be published.
(49) Note that $F_{des} \approx 35$ pN was found for the desorption of lowly charged PVA(10%) from hydrophobized silica.
(50) Vigil, G.; Xu, Z.; Steinberg, S.; Israelachvili, J. *J. Colloid Interface Sci.* **1994**, *165*, 367−385.
(51) Pashley, R. M. *J. Colloid Interface Sci.* **1981**, *83*, 531−546.

MA0009404